

Supplementary Information

Theoretical Understanding and Prediction of Metal-doped CeO₂ Catalyst for Ammonia Dissociation

Yongjie Shen,^a Kaewraung Wongsathorn,^b and Min Gao ^{*a}

^aInstitute for Chemical Reaction Design and Discovery (WP-ICReDD), Institute for Catalysis Hokkaido University, Sapporo 001-0021, Japan.

^b Graduate School of Chemical Sciences and Engineering, Hokkaido University, Sapporo 060-8628, Japan.

*To whom correspondence should be corresponded: gaomin@icredd.hokudai.ac.jp

This pdf file includes:

Table S1 to S4 (page S3-S6)

Fig S1 to S12 (pages S7-S18)

Content

Table S1 U_{eff} (eV) value of transition metal elements	S3
Table S2 Distance between the doping metal and oxygen	S4
Table S3 Relevant properties calculated by DFT for metal and metal-doped catalysts	S5
Table S4 Adsorption energies of NH_3 -related species on metal-doped CeO_2	S6
Figure S1 Relative energies of Ni-doped, V-doped, and Nb-doped CeO_2 surfaces and the structures of adsorbed species (NH_3 , $\text{NH}_2\text{-H}$, $\text{NH}_2\text{-H}$ and N_3H) on the corresponding surfaces at different k-point mesh density	S7
Figure S2 Structural diagrams of pure CeO_2 and CeO_2 doped with different transition metals..	S8
Figure S3 Adsorption structures of NH_3 , $\text{NH}_2\text{-H}$, $\text{NH}_2\text{-H}$ and N_3H on metal (V, Cr, Mn, Fe, and Co)-doped CeO_2	S9
Figure S4 Adsorption structures of NH_3 , $\text{NH}_2\text{-H}$, $\text{NH}_2\text{-H}$ and N_3H on metal (Ni, Cu, Zn, Nb, Tc, and W)-doped CeO_2	S10
Figure S5 Valence band maximum as function of the adsorption energies of $\text{NH}_2\text{-H}$ species in NH_3 dissociation.....	S11
Figure S6 Oxygen vacancy formation as function of the adsorption energies of (a) NH_3 , (b) $\text{NH}_2\text{-H}$, (c) $\text{NH}_2\text{-H}$, and (d) N_3H species in NH_3 dissociation.....	S12
Figure S7 Valence band maximum as function of the activation energies for the transition states of (a) $\text{NH}_3 \rightarrow \text{NH}_2\text{-H}$, (b) $\text{NH}_2\text{-H} \rightarrow \text{NH}_2\text{-H}$, and (c) $\text{NH}_2\text{-H} \rightarrow \text{N}_3\text{H}$ in NH_3 dissociation	S13
Figure S8 Schematic diagram of the interaction between HOMO and LUMO	S14
Figure S9 The Linear relationship between NH_3 adsorption energy and $\Delta E_{\text{LUMO}(\text{Metal})-\text{HOMO}(\text{N})}$	S15
Figure S10 Work function as function of the adsorption energies of (a) NH_3 , (b) $\text{NH}_2\text{-H}$, and (c) $\text{NH}_2\text{-H}$ species in NH_3 dissociation	S16
Figure S11 Valence band maximum as function of the work function.....	S17
Figure S12 (a) Valence band maximum, (b) work function, and (c) highest oxidation state as function of the adsorption energies of H	S18
Reference	S19

Element	Sc	Ti	V	Cr	Mn	Fe	Co	Ni	Cu	Zn	Y
U_{eff} (eV)	5.0	4.2	3.1	3.5	4.5	4.0	3.4	6.0	6.0	8.0	3.5
Ref	1	2	3	4	5	6	4	4	7	8	9
Element	Zr	Nb	Mo	Tc	Cd	La	Ce	Pr	Nd	Sm	W
U_{eff} (eV)	4.0	4.0	3.5	-	2.0	5.0	5.0	4.5	6.0	-	6.2
Ref	10	11	4		12	13	14	15	16		17

Table S1 U_{eff} (eV) value of transition metal elements.

Table S2 Distance between the doping metal and oxygen.

	Metal-oxygen distance (Å)						
	distance1	distance 2	distance 3	distance 4	distance 5	distance 6	distance 7
V	2.131	1.962	1.960	1.698	3.121	3.436	2.041
Cr	2.889	1.803	1.876	1.806	2.870	3.452	1.909
Mn	2.467	2.636	2.110	2.812	2.098	2.390	2.208
Fe	2.633	2.055	2.125	2.025	2.836	2.053	2.082
Co	1.780	3.680	3.357	3.666	1.774	1.757	1.868
Ni	1.805	1.848	1.805	3.662	3.385	3.690	1.887
Cu	1.839	3.705	3.324	3.684	1.837	1.841	1.878
Zn	1.997	3.501	2.010	3.517	1.995	3.191	1.955
Nb	2.580	1.942	2.424	1.941	2.602	1.950	2.005
Tc	2.646	1.790	2.745	1.787	2.694	1.757	1.903
W	2.428	1.837	2.399	1.837	2.869	1.825	1.924

Table S3 Relevant properties calculated by DFT for metal and metal-doped catalysts.

	E_{SMA}^a (eV)	BG^b (eV)	DBC^c (eV)	VBM^d (eV)	CBM^e (eV)	WF^f (eV)	E_{dope}^g (eV)
V	-6.43	1.21	-0.27	-0.51	0.70	4.96	3.39
Cr	-5.91	1.80	0.14	-1.10	0.70	5.60	4.41
Mn	-6.82	0.56	-3.04	-1.25	-0.68	5.76	7.24
Fe	-5.45	0.93	-1.69	-1.16	-0.23	5.76	7.29
Co	-4.71	0.22	-2.38	-1.37	-1.15	5.94	8.29
Ni	-2.40	0.34	-3.16	-1.43	-1.09	6.17	9.03
Cu	-2.39	0.27	-3.84	-1.44	-1.17	6.22	10.48
Zn	-0.79	0.61	-6.97	-1.42	-0.81	5.94	8.98
Nb	-7.34	0.43	-4.14	0.33	0.76	4.35	0.96
Tc	-10.99	0.11	-3.64	0.43	0.54	4.49	5.76
W	-13.64	0.55	-3.20	0.22	0.77	4.39	2.64

A: the energy of single metal atom. *b*: band gap. *C*: d band center. *D*: valence band maximum. *E*: conduction band minimum. *F*: work function.

G: the energy of doping formation.

Table S4 Adsorption energies of NH₃-related species on metal-doped CeO₂.

	E_{NH_3} (eV)	$E_{\text{NH}_2\text{-H}}$ (eV)	$E_{\text{NH}_2\text{-H}}$ (eV)	$E_{\text{N-3H}}$ (eV)	E_{H} (eV)
V	-0.67	-1.26	-1.41	-1.42	-3.58
Cr	-0.54	-1.36	-1.44	-1.47	-4.23
Mn	-1.62	-1.81	-2.10	-1.98	-4.96
Fe	-0.40	-1.54	-0.70	0.14	-5.17
Co	-1.35	-1.47	-1.13	-1.49	-4.94
Ni	-1.62	-1.49	-1.76	-1.56	-5.22
Cu	-1.09	-1.09	-1.35	-1.66	-5.24
Zn	-1.38	-1.48	-1.91	-1.95	-5.09
Nb	-0.36	-0.90	-0.22	0.51	-3.91
Tc	0.23	0.15	-0.59	-2.48	-3.07
W	-0.05	-0.33	-0.29	0.29	-3.40

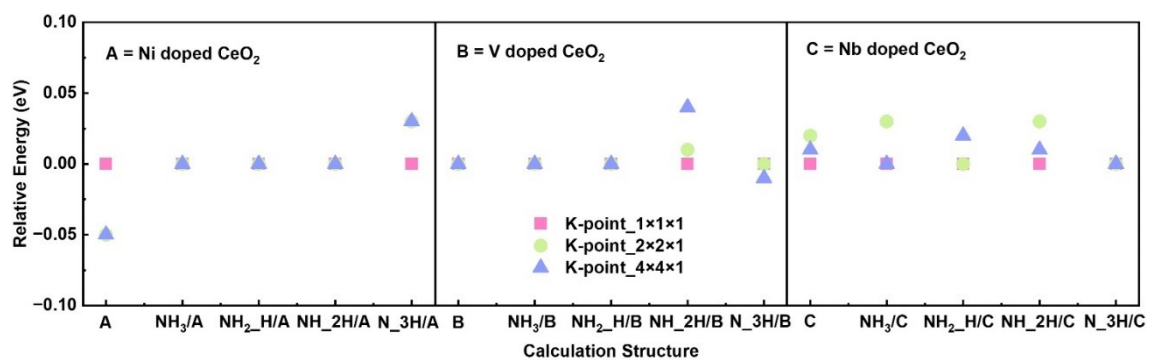


Figure. S1 Relative energies of Ni-doped, V-doped, and Nb-doped CeO₂ surfaces and the structures of adsorbed species (NH₃, NH₂_H, NH_2H and N_3H) on the corresponding surfaces at different k-point mesh density.

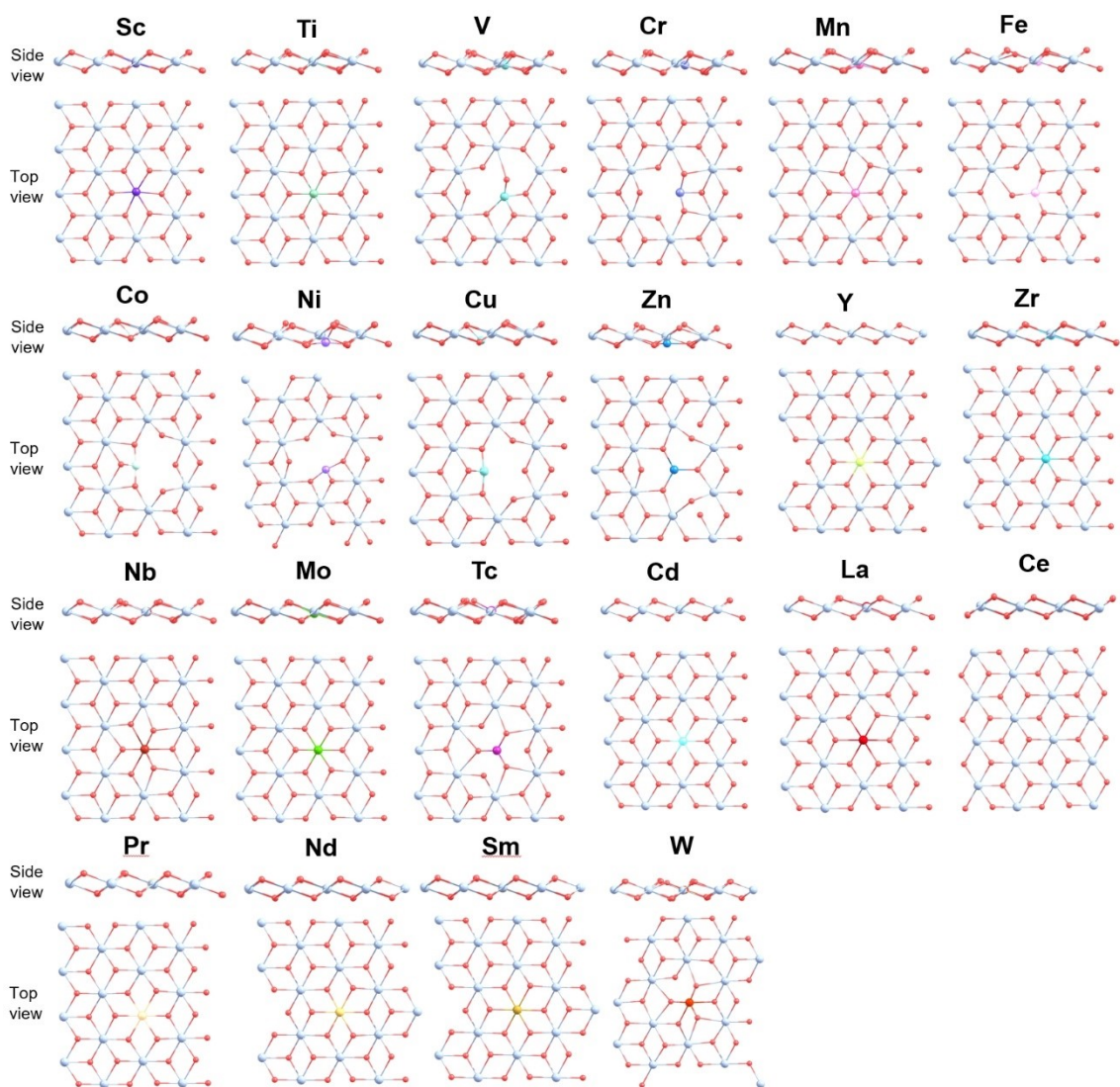


Figure. S2 Structural diagrams of pure CeO₂ and CeO₂ doped with different transition metals.

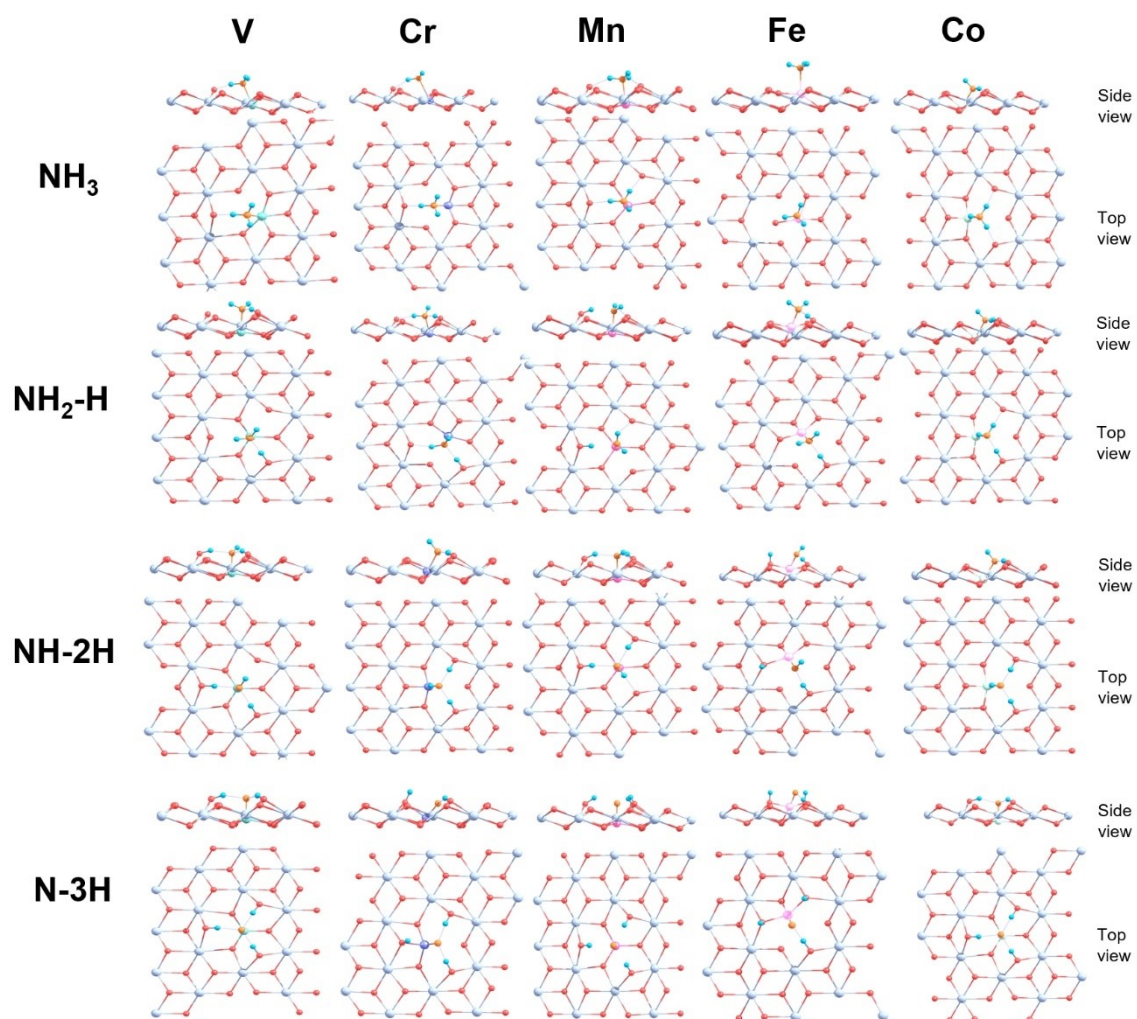


Figure. S3 Adsorption structures of NH₃, NH₂-H, NH-2H and N-3H on metal (V, Cr, Mn, Fe, and Co)-doped CeO₂.

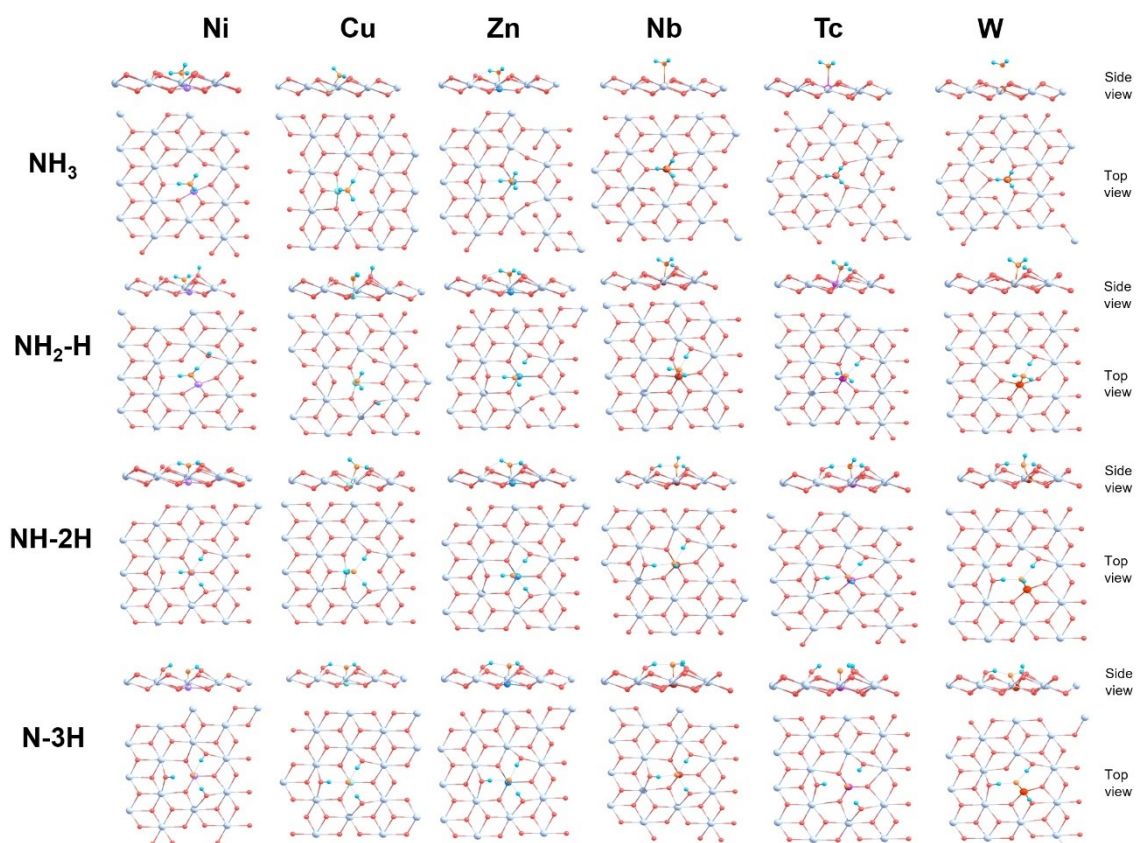


Figure. S4 Adsorption structures of NH₃, NH₂-H, NH-2H and N-3H on metal (Ni, Cu, Zn, Nb, Tc, and W)-doped CeO₂.

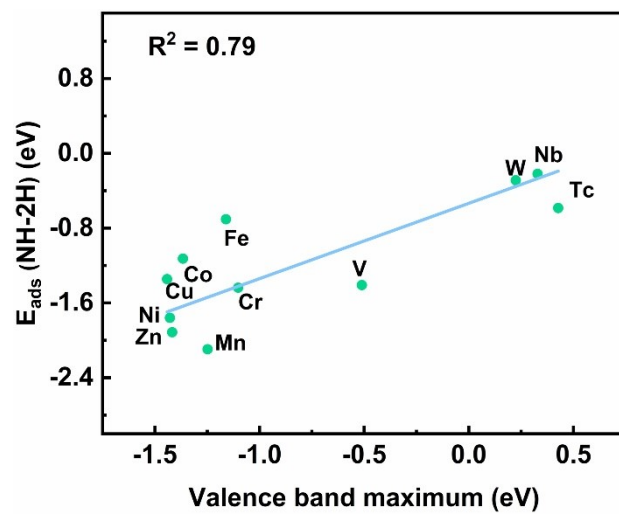


Figure. S5 Valence band maximum as function of the adsorption energies of NH₂-H species in NH₃ dissociation.

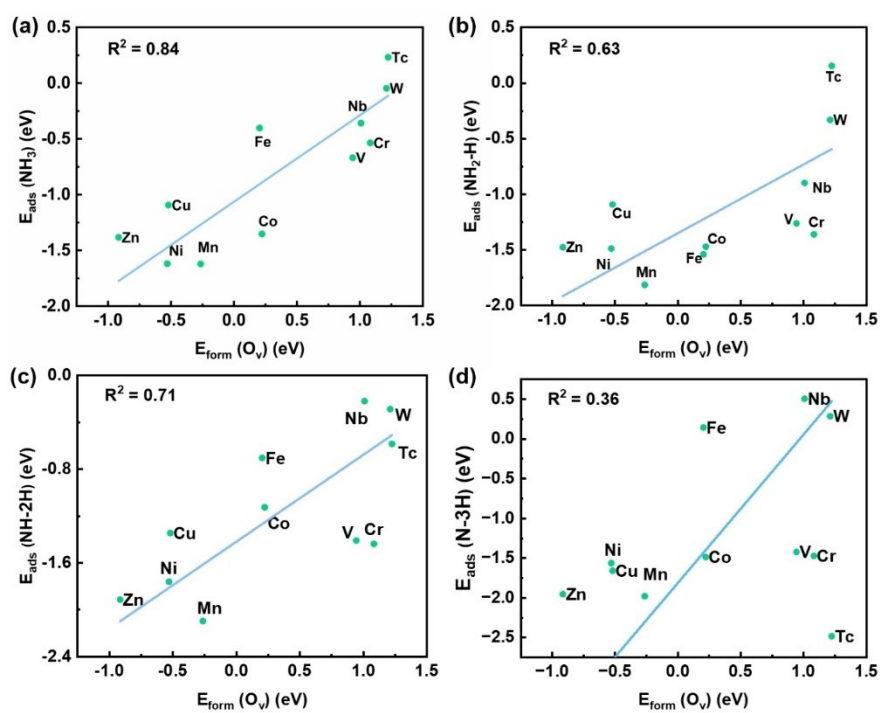


Figure. S6 Oxygen vacancy formation as function of the adsorption energies of (a) NH_3 , (b) $\text{NH}_2\text{-H}$, (c) NH-2H , and (d) N-3H species in NH_3 dissociation.

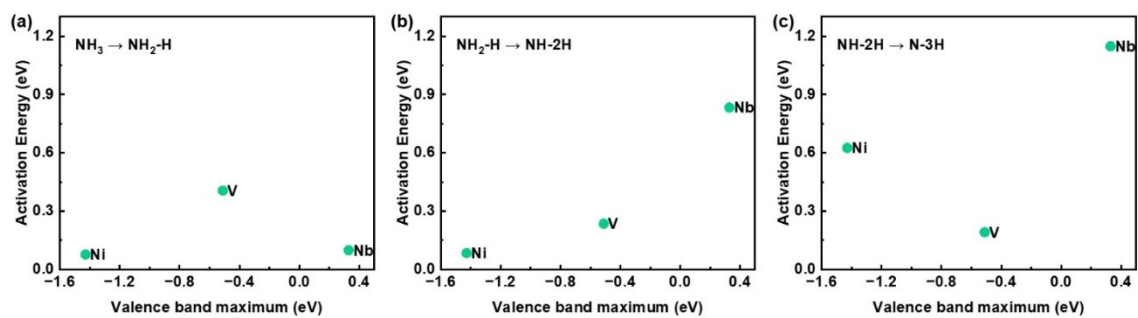


Figure. S7 Valence band maximum as function of the activation energies for the transition states of (a) $\text{NH}_3 \rightarrow \text{NH}_2\text{-H}$, (b) $\text{NH}_2\text{-H} \rightarrow \text{NH-2H}$, and (c) $\text{NH-2H} \rightarrow \text{N-3H}$ in NH_3 dissociation.

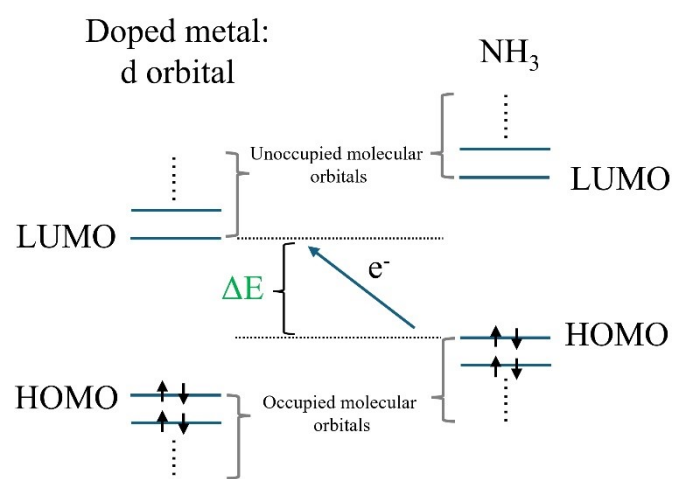


Figure. S8 Schematic diagram of the interaction between HOMO and LUMO.

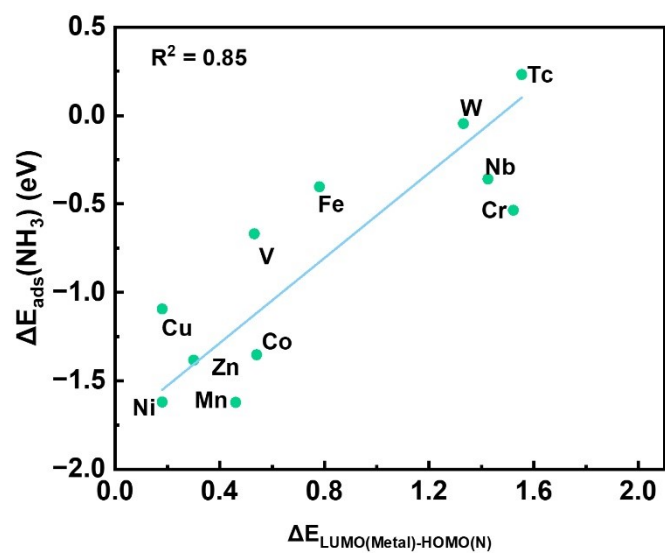


Figure. S9 The Linear relationship between NH₃ adsorption energy and $\Delta E_{\text{LUMO}(\text{Metal})-\text{HOMO}(\text{N})}$ (the difference between the LUMO energy of doped metal d orbital and the HOMO energy of N p orbital in NH₃).

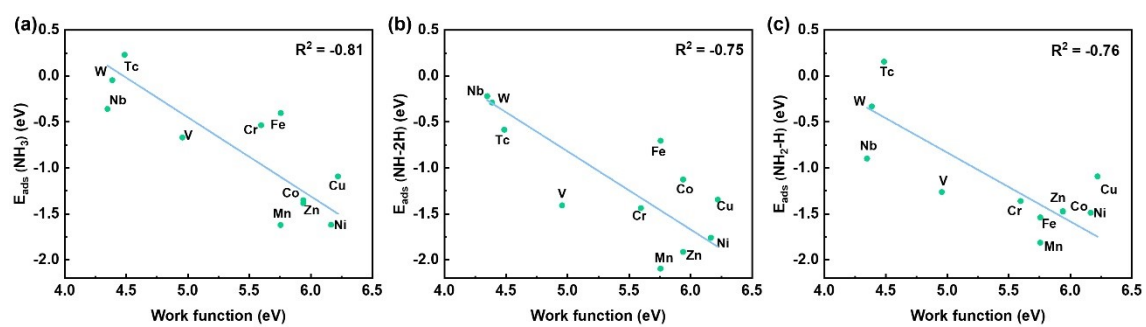


Figure. S10 Work function as function of the adsorption energies of (a) NH_3 , (b) $\text{NH}_2\text{-H}$, and (c) $\text{NH}_2\text{-H}$ species in NH_3 dissociation.

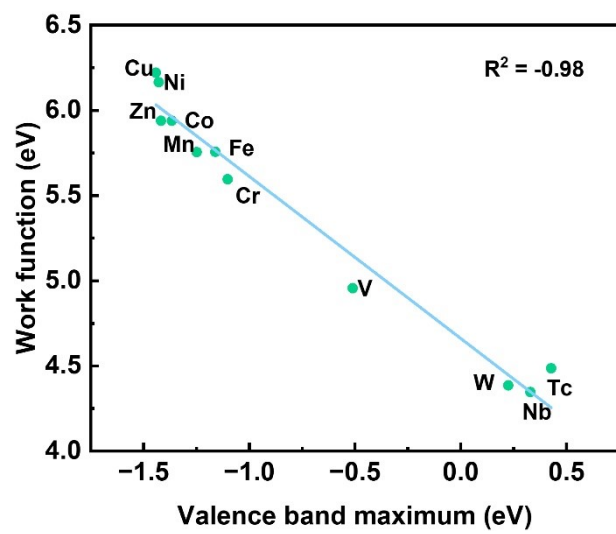


Figure. S11 Valence band maximum as function of the work function.

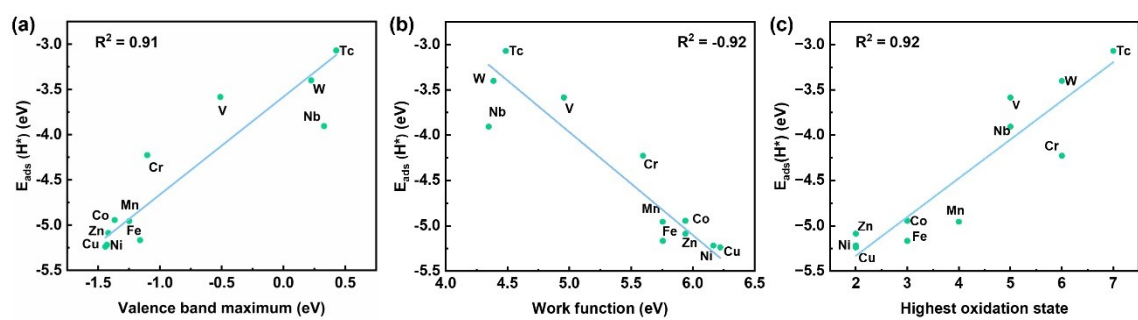


Figure. S12 (a) Valence band maximum, (b) work function, and (c) highest oxidation state as function of the adsorption energies of H.

- 1 Q. Meng, T. Wang, E. Liu, X. Ma, Q. Ge and J. Gong, *Phys. Chem. Chem. Phys.*, 2013, **15**, 9549-9561.
- 2 F. Liu, H. He, Y. Ding and C. Zhang, *Appl. Catal. B Environ. Energy*, 2009, **93**, 194-204.
- 3 G. Sai Gautam, P. Canepa, A. Abdellahi, A. Urban, R. Malik and G. Ceder, *Chem. Mater.*, 2015, **27**, 3733-3742.
- 4 A. Jain, G. Hautier, S. P. Ong, C. J. Moore, C. C. Fischer, K. A. Persson and G. Ceder, *Phys. Rev. B*, 2011, **84**, 045115.
- 5 W. Song, J. Liu, H. Zheng, S. Ma, Y. Wei, A. Duan, G. Jiang, Z. Zhao and E. J. M. Hensen, *Catal. Sci. Technol.*, 2016, **6**, 2120-2128.
- 6 R. Grau-Crespo, F. Corà, A. A. Sokol, N. H. de Leeuw and C. R. A. Catlow, *Phys. Rev. B*, 2006, **73**, 035116.
- 7 B. Himmetoglu, R. M. Wentzcovitch and M. Cococcioni, *Phys. Rev. B*, 2011, **84**, 115108.
- 8 S. Haffad and K. Korir Kiprono, *Surf. Sci.*, 2019, **686**, 10-16.
- 9 B. Saha, T. D. Sands and U. V. Waghmare, *J. Appl. Phys.*, 2011, **109**, 073720.
- 10 Y. Tang, S. Zhao, B. Long, J.-C. Liu and J. Li, *J. Phys. Chem. C*, 2016, **120**, 17514-17526.
- 11 Y. Fang, D. Cheng, M. Niu, Y. Yi and W. Wu, *Chem. Phys. Lett.*, 2013, **567**, 34-38.
- 12 L. N. Bai, B. J. Zheng, J. S. Lian and Q. Jiang, *Solid State Sciences*, 2012, **14**, 698-704.
- 13 S. Grieshammer, M. Nakayama and M. Martin, *Phys. Chem. Chem. Phys.*, 2016, **18**, 3804-3811.
- 14 Z. Su, X. Li, W. Si, L. Artiglia, Y. Peng, J. Chen, H. Wang, D. Chen and J. Li, *ACS Catal.*, 2023, **13**, 3444-3455.
- 15 B. Milberg, A. Juan and B. Irigoyen, *Appl. Surf. Sci.*, 2017, **401**, 206-217.
- 16 K. O. Obodo, G. Gebreyesus, C. N. M. Ouma, J. T. Obodo, S. O. Ezeonu, D. P. Rai and B. Bouhafs, *RSC Adv.*, 2020, **10**, 15670-15676.
- 17 J. Tao, Q. Zhang and T. Liu, *Phys. Chem. Chem. Phys.*, 2022, **24**, 22918-22927.

References